AD-A071 454 ROYAL AUSTRALIAN NAVY RESEARCH LAB EDGECLIFF F/G 17/9
ON SURFACE-BASED ADVECTIVE RADAR DUCTS.(U)
DEC 78 P J MULHEARN
UNCLASSIFIED RANRL-TN-5/78 NL

| OF |
AD
A071454

END
DATE
FILMED
9-79
DDC

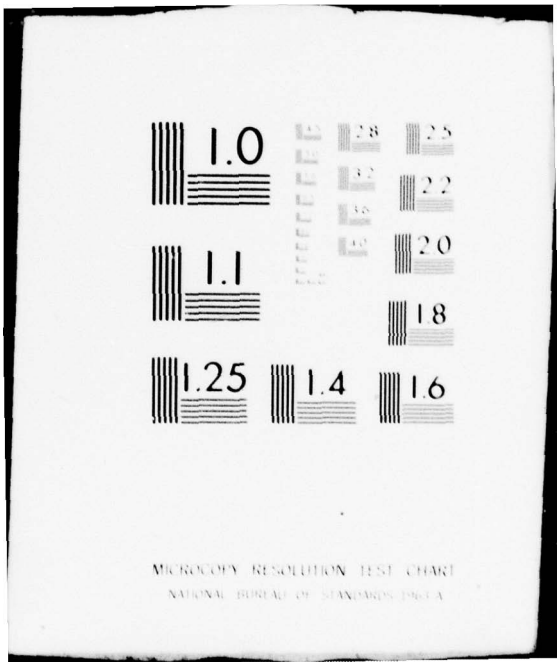
1.0
1.1
1.25
1.4
1.6
2.8
2.5
3.2
2.2
3.6
2.0
4.0
1.8
MICROCOPY RESOLUTION TEST CHART
NATIONAL BUREAU OF STANDARDS 1963-A

UNCLASSIFIED

AR Number: AR-001-030

DEPARTMENT OF DEFENCE
DEFENCE SCIENCE AND TECHNOLOGY ORGANISATION
R.A.N. RESEARCH LABORATORY
EDGECLIFF, N.S.W.

RANRL TECHNICAL NOTE 5/78

ON SURFACE-BASED ADVECTIVE RADAR DUCTS (U)

BY

P. J. MULHEARN

APPROVED FOR PUBLIC RELEASE

COPY No. 8

DECEMBER 1978

UNCLASSIFIED

DEPARTMENT OF DEFENCE

RAN RESEARCH LABORATORY

RANRL TECHNICAL NOTE 5/78

ON SURFACE-BASED ADVECTIVE RADAR DUCTS

P. J. Mulhearn

S U M M A R Y

As a warm, well mixed air mass flows off a land surface and over a cooler sea, the air is modified in a layer near the surface. Within this layer humidity decreases while temperature increases with height and a radar duct is formed. The non-dimensional parameters governing the growth of the modified layer are derived and simple forms are found for the increase of layer height with fetch and for the shapes of humidity and temperature profiles. From these relations the depth and strength of the radar duct are derived as functions of the modified layer depth and the differences in potential temperature and water vapour pressure between the over-land air mass and air in thermodynamic equilibrium with the sea-surface.

Approved for Public Release.

POSTAL ADDRESS: The Superintendent, RAN Research Laboratory
P.O. Box 706, Darlinghurst N.S.W. 2010

DOCUMENT CONTROL DATA SHEET

Security classification of this page: UNCLASSIFIED

1. DOCUMENT NUMBERS:
   a. AR Numbers: 001 030
   b. Document Series: (9) RANRL Technical Note
   c. Report Number: 5/78

2. SECURITY CLASSIFICATION:
   a. Complete document: UNCLASSIFIED
   b. Title in isolation: UNCLASSIFIED
   C. Summary in Isolation: UNCLASSIFIED

3. TITLE:
(6) ON SURFACE-BASED ADVECTIVE RADAR DUCTS. (11) (12) 28 p.

4. PERSONAL AUTHOR(S):
(10) Mulhearn, Phillip J. / Mulhearn

5. DOCUMENT DATE: Dec[redacted], 1978

6. TYPE OF REPORT AND PERIOD COVERED:
Progress; 1978

7. CORPORATE AUTHOR(S):
RAN Research Laboratory
P.O. Box 706
Darlinghurst NSW 2010

8. REFERENCE NUMBERS:
   a. Task: NAV Task 76/60
   b. Sponsoring Agency: NSA
   c. Approved [redacted] SSRL

(14) RANRL-TN-5/78

9. COST CODE:

10. IMPRINT (Publishing establishment):
RAN Research Laboratory

11. COMPUTER PROGRAM(S) (Title(s) and language(s)):
NIL

12. RELEASE LIMITATIONS (of the document in addition to the Distribution List)

AUSTRALIA: Approved for Public Release.

OVERSEAS: N.O. | P.R. 1 | A | B | C | D | E

13. ANNOUNCEMENT LIMITATIONS (of the information on this page):

No limitation

14. DESCRIPTORS:
Fluid Mechanics
Radar detection
Atmospheric Physics

15. COSATI CODES:
2004
1709
0401

16. SUMMARY: As a warm, well mixed air mass flows off a land surface and over a cooler sea, the air is modified in a layer near the surface. Within this layer humidity decreases while temperature increases with height and a radar duct is formed. The non-dimensional parameters governing the growth of the modified layer are derived and simple forms are found for the increase of layer height with fetch and for the shapes of humidity and temperature profiles. From these relations the depth and strength of the radar duct are derived as functions of the modified layer depth and the differences in potential temperature and water vapour pressure between the overland air mass and air in thermodynamic equilibrium with the sea surface.

UNCLASSIFIED
Security classification of this page

DISTRIBUTION LIST

	Copy No.
Chief Defence Scientist	1
Deputy Chief Defence Scientist	2
Assistant Secretary, Science & Technology Administration	3
Controller, Service Laboratories & Trials Division	4
Joint Intelligence Organisation (DDSTI)	5
Defence Library, Campbell Park	6
Defence Information Services Branch - Microfiche	7
- release to US - DDC	8 - 19
- release to UK - DRIC	20
- release to Canada - DSIS	21
- release to NZ - DoD	22
Director, Naval Meteorological & Oceanographic Services	23
Deputy Director, Naval Meteorological & Oceanographic Services	24
Mr Neil Jones, Defence Research Centre Salisbury	25
Library, RAN Research Laboratory	26 - 36
Library, DRCS	37
Library, CSIRO Division of Atmospheric Physics	38
Prof J.S. Turner, A.N.U., Research School of Earth Sciences	39

CONTENTS

List of Symbols

a = radius of the earth

b = $4800^{o}K$, a constant in equation (7)

c = $79^{o}K/mb$, a constant in equation (7)

e_p = potential water vapour pressure

e_{p1} = upstream potential water vapour pressure

$e_w(T_o)$ = water vapour pressure in equilibrium with the sea surface.

f = $(1 - (z/h)^{\frac{1}{4}})$

g = acceleration due to gravity

g' = $g\Delta\rho/\rho$

h = height of modified layer

m = number of trapped modes

M = refracrive modulus

N = refractive index

p = pressure

p_o = atmospheric surface pressure

R = $b \Delta e p /(p_o \Delta \theta)$

s = slope of curve of equilibrium water vapour pressure above a sea surface versus temperature.

S = $\frac{c}{\theta_1^2} (p_o \Delta \theta - b \Delta e p)$

T = temperature

T_o = sea-surface temperature

T_s = dew-point temperature

T_{s1} = upstream dew-point temperature

U = upstream wind speed

x = fetch over the sea surface

z = height above the sea surface

z_D = height of radar duct when $z_d < h$

z_o = aerodynamic roughness of sea surface

Δe_p = $e_{p1} - e_w(T_o)$

ΔT_s = $T_{s1} - T_o$

γ = adiabatec lapse rate $\simeq 10^{-2}$ $^{o}C/m$

ρ = air density

Φ = potential refracrive modulus

θ = potential temperature

θ_1 = upstream potential temperature

$\Delta\rho$ = difference in density between air at the sea surface and air upstream

$\Delta\theta$ = $\theta_1 - T_o$

1. INTRODUCTION

Radar ranges can be greatly enhanced by the formation in the atmosphere of temperature and humidity profiles which cause a decrease with height over some interval of the radio refractive index, and the consequent formation of a radar duct. Such conditions will result from an increase in temperature and/or a decrease in humidity with height.

It would be desirable to establish the probability of occurrence of radar ducting conditions over the sea in areas around Australia from available meteorological statistics, and to be able to predict such conditions from synoptic weather forecasts.

To do either of these tasks requires a greater understanding of the physical factors involved.

Radar ducts over the sea may be divided into three main types:

a. Advective ducts - formed, for example, when warm air from the land blows over a cooler sea causing humidity to decrease and temperature to increase with height.

b. Evaporative duct - formed when high evaporation rates from the sea cause sharp, surface based humidity gradients.

c. Elevated ducts, principally at subsidence inversions where a sinking dry air mass is separated from a lower, moister and cooler air mass by a sharp interface.

Advective and evaporation ducts are both surface based. The physical understanding of evaporation ducts when advective effects are absent is well advanced, but the prevalence of their occurrence in waters near Australia still needs to be worked out.

Quantitative prediction of elevated ducts is a major scientific problem. However in tropical waters where the trade wind inversion appears to be a stable feature of the atmosphere a series of descriptive measurements could be useful. An elevated layer can also be formed by advection of dry air off a land mass and over a warmer sea surface. Under these conditions buoyant convection will often mix the air very well up to some level at which there will be sharp gradients in temperature and humidity. A fuller discussion of types of radar duct may be found in Lane and others (1976).

This note is concerned with the formation of surface-based advective ducts caused by advection of a warm, homogeneous air mass over a cooler sea surface. It is restricted to steady state conditions. Extensive experimental data are available for this situation in reports of experiments performed in 1944 over the waters of Massachusetts Bay, USA. (Craig, 1946, 1949; Kerr, 1951, Chp 3). A summary of the data is presented in Table 1. Although these are old data they are still the best available. Measurements were obtained of humidity and temperature profiles and of the radar propagation associated with these profiles. Full details are available in the above references. This note is mainly concerned with the temperature and humidity profiles and does not address the propagation problem in much detail.

Advective ducts of the type considered here should be common off the north-west coast of Australia in daylight hours in the cooler half of the year. The prevailing winds are offshore and the air will be dry and hotter than the sea for much of the day. The distance out to sea to which the ducts persist is unknown but from the available data should be at least 100 km.

2. THEORY

Over land in reasonably sunny weather the air is often well-mixed up to a height of the order of 1 km by buoyant convection. Under such conditions the potential temperature, θ_l [+] and potential dew point, T_{sl}, are constant within the above height interval except for a region of large gradients in a thin region close to the ground. Under these conditions the wind speed, U, and its direction are also approximately constant with height. When such a well-mixed air mass moves over a cooler sea-surface, with constant temperature, T_o, a layer of depth, h, forms in which the potential temperature θ, is decreased and the potential dew point, T_s, increased relative to their overland values. The growth with fetch, x, of the modified layer of height h, depends on the aerodynamic roughness, z_o, of the sea-surface, the wind-speed, and the change in buoyancy between the air over

---

[+] In the homogeneous air mass the temperature, T, decreases with height, at the adiabatic lapse rate of approximately $1^{o}C/100$ m, because pressure falls with height. The potential temperature θ is constant with height in a homogeneous air mass and T is related to θ by

$$\theta = T + \gamma z \ .$$

where γ = the adiabatic lapse rate $\simeq 10^{-2}\ ^{o}C/m$.
A similar relation applies for dew point.

the land and that in contact with the sea-surface. That is

$$h = \text{function}\left(\frac{g\Delta\rho}{\rho}, u, x, z_o\right) \quad \ldots\ (1)$$

where g = acceleration due to gravity,

$\Delta\rho$ = difference in density between air at the sea surface and air upstream,

ρ = average air density .

Equation (1) may be written in two alternative forms:

$$h/x = \text{function}\left(\frac{g\Delta\rho x}{\rho u^2}, z_o/x\right) \quad \ldots\ (2)$$

$$\text{or} \quad \frac{g\Delta\rho h}{\rho u^2} = \text{function}\left(\frac{g\Delta\rho x}{\rho u^2}, z_o/x\right) \quad \ldots\ (3)$$

It can be shown (Krauss 1972, p 50) that

$$\frac{\Delta\rho}{\rho} = -\frac{(\theta_1 - T_o)}{T} - \frac{3\Delta e_p}{8p} ,$$

where Δe_p = (potential water vapour pressure upstream) - (water vapour pressure of air in thermodynamic equilibrium at the sea surface temperature).

Note that, if the upstream air is relatively hot and dry, $(\theta_1 - T_o)$ and Δe_p are the opposite sign, so that if the former is small, $\frac{\Delta\rho}{\rho}$ may be negative and then air within the modified layer will be less dense than that aloft, causing mixing by bouyant convection. This paper is only concerned with cases where $\Delta\rho/\rho > 0$. Usually $\frac{3\Delta e}{8p} \simeq 0.1\,\frac{\Delta T_s}{T}$, where ΔT_s is the difference between the upstream potential dew-point temperature and the sea-surface temperature, and in most of the available experiments ΔT_s is of order 10% of $(\theta_1 - T_o)$.

The sea surface has very low aerodynamic roughness under most conditions, and in the absence of advective effects vertical gradients of all quantities are small. For this reason the influence of z_o will be assumed negligible from now on and (2) and (3) simplify to

$$h/x = \text{function}\left(\frac{g'x}{u^2}\right) \quad \ldots\ (4)$$

$$\text{and } g'h/u^2 = \text{function}\left(\frac{g'x}{u^2}\right) \quad \ldots\ (5)$$

where $g' = g\Delta\rho/\rho$.

In fig 1 values of h obtained from the profiles of Craig (1946) and Kerr (1951) are plotted against x. Note that even at a fetch of 100 km, h is only of the order of 200 m. The main uncertaincies in h arise from the difficulty of determining the exact point at which temperature or humidity values from within the modified layer reach the values in the homogeneous outer flow. A second difficulty is that this point is sometimes different for humidity and temperature. These two problems occur more often at longer ranges and suggest that other processes apart from simple modification by the cool sea-surface may play a role, especially as fetch increases. In addition turbulent fluctuations within the modified layer, which will cause fluctuations in the edge of the layer, will have larger time and space scales at larger fetches and will thus be harder to average out. It can be seen from fig 1 that the scatter between experimental points is greater than the uncertainty in the data.

In fig 2, where $g'h/u^2$ is plotted against $g'x/u^2$, this scatter is greatly reduced. The two circled points had an overwater fetch of only 4.8 km and lie above the rest of the data which has fetches greater than 12 km. There are less data in fig 2 than in fig 1, because wind-speed was always measured only at 1000 ft (305 m), and in the omitted experiments an inversion layer occurred below 300 m but above the top of the modified layer. Under these conditions the wind speed at 300 m will not be an appropriate value for scaling purposes, because its relation to winds below the inversion is complex. Figure 2 is presented as a comparison with fig 1. If the points omitted in fig 2 are ommitted from fig 1 the scatter in the latter is not reduced. However in fig 2 (g'/u^2) occurs on both axes. A better presentation is that of fig 3, where (h/x) is shown versus $(g'x/u^2)$.

The straight line through the points in fig 2 is

$$\frac{g'h}{u^2} = 0.014 \left(\frac{g'x}{u^2} \right)^{0.55} .$$

From the error bars in fig 2 the exponent could lie within ± 25% of 0.55 but these limits are extreme values. It is more plausible that 0.55 is accurate within 10%. The straight line in fig 3 is

$$h/x = 1.46 \times 10^{-2} \left(\frac{g'x}{u^2} \right)^{-0.47} \qquad \ldots.(6)$$

This exponent is also most likely accurate within ± 10%. These are both

empirical relations obtained by drawing a "best-fit" straight line through the data by eye. Calculating a least squares fit is not warranted at this stage.

For predictions of radar propagation not only the depth of the modified layer but the shapes of temperature and humidity profiles within that layer are required.

In many turbulent flows mean profiles are self-preserving or approach a self-preserving form at a sufficiently large distance downstream where they are no longer influenced by the upstream boundary conditions. A self-preserving form is one in which the shape of a profile remains constant with fetch if it is suitably non-dimensionalised. The most obvious scaling parameters for potential dew point and temperature profiles are the height of the modified layer, h, the differences, ΔT_s, between the upstream potential dew point and the sea-surface temperature, and for temperature profiles, the difference $(\theta_1 - T_o)$.

Figure 4 humidity data are presented for $x \gtrsim 16$ km, as profiles of potential dew point temperature T_s versus height. They are presented in the normalised form $(T_s - T_o) / \Delta T_s$ versus z/h. There is a fair amount of scatter in these profiles but no trend with x or $g'x/u^2$ was discernable for $x \gtrsim 16$ km. The dashed line through the data is

$$(T_s - T_o) / \Delta T_s = (z / h)^{1/4} ,$$

and this provides a good fit through both the potential dew point and potential temperature profiles. All the data fall between bounds given by $(z/h)^{1/3}$ and $(z/h)^{1/5}$. The temperature profiles are presented in fig 5, for $x \gtrsim 16$ km, and are very similar to the dew point profiles.

Profiles of temperature and dew point at shorter fetches are presented in fig 6. These lie to the right of the profiles presented in figs 4 and 5. The fetch required for the shape of temperature and humidity profiles to approach an equilibrium state, if one exists, will depend on the detailed boundary conditions at the upstream land-sea interface (eg depth of the overland super-adiabatic layer, cliffs). These conditions are only poorly known in practice. The division chosen here at 16 km is somewhat arbitrary and is based only on an empirical investigation of the available data.

To summarise, it has been seen that h/x = function $(g'x/u^2)$ and empirically $h/x = 1.46 \times 10^{-2}(g'x/u^2)^{-0.47}$, for $x > 5$ km, and that potential temperature and potential dew-point profiles for $x \geq 16$ km have the forms

$$(\theta - T_o) / (\theta_1 - T_o) = (z/h)^{\frac{1}{4}}$$

$$(T_s - T_o) / \Delta T_s = (z/h)^{\frac{1}{4}} .$$

Further experiments are required to test the downstream fetch to which the above rules apply. Within 100 km of a coastline the available evidence suggests they are reasonably good and can be used as a basis for deriving refractive index profiles.

3. PROFILES OF REFRACTIVE MODULUS

The refractive modulus $M(z)$ is defined by

$$M(z) = (N(z) - 1)10^6 + z/a.$$

where $N(z)$ = refractive index

z = height, and

a = the radius of the earth.

In a homogeneous air mass M varies linearly with height, with a gradient of approximately $0.13\ m^{-1}$ (Kerr, 1951) and the potential refractive modulus Φ is constant, so that $M = \Phi + 0.13\ z$.

From Kerr (1951)

$$\Phi = \frac{c}{\theta}\left(p_o + b\,\frac{e_p}{\theta} \right) , \qquad \ldots.(7)$$

where θ is the potential temperature,

e_p is the potential water bapour pressure

p_o is surface atmospheric pressure ,

and c and b are constants with $c = 79^{\circ}K/mb$ and $b = 4800^{\circ}K$.

(In inhomogeneous air Φ , θ , and e_p are function of height z.)

In an advective duct it was found above that

$$\theta = T_o + \Delta\,\theta\,(z/h)^{\frac{1}{4}} \qquad \ldots.(8)$$

where $\Delta\theta = \theta_1 - T_o$ and

$$T_s - T_o = \Delta\,T_s(z/h)^{\frac{1}{4}}$$

But $(T_s - T_o) \doteq |e_p - e_w(T_o)|/s$,

and $\Delta T_s \doteq |e_{p1} - e_w(T_o)|/s = \Delta e_p/s$

so that $e_p = e_w(T_o) + \Delta e_p \, (z/h)^{1/4}$, ...(9)

where e_{p1} = upstream potential water vapour pressure,

$e_w(T_o)$ = water vapour pressure of air in equilibrium with the sea surface,

and s = the slope of the equilibrium water vapour pressure versus temperature curve over a sea-surface.

Equation (8) and (9) may be rearranged so that

$$\theta = \theta_1 - \Delta\theta\left[1 - (z/h)^{1/4}\right]$$

and ....(10)

$$e_p = e_{p_1} - \Delta e_p\left[1 - (z/h)^{1/4}\right]$$

Put $\left[1 - (z/h)^{1/4}\right] = f$, and substitute equation (10) into equation (7).

Then $$\Phi = \frac{c}{\theta_1 - \Delta\theta f}\left(p_o + f\,\frac{e_{p1} - \Delta e_p f}{\theta_1 - \Delta\theta f}\right) .$$

Assuming $\Delta\theta << \theta_1$, this simplifies to

$$\Phi \simeq \Phi_1 - \frac{c}{\theta_1}\left[\frac{b\,\Delta e_p}{\theta_1} - \frac{\Delta\theta\, p_o}{\theta_1}\right]\left\{1 - (z/h)^{1/4}\right\} ,$$

where $\Phi_1 = \frac{c}{\theta_1}\left(p_o + \frac{b\, e_{p1}}{\theta_1}\right)$, the upstream potential refractive modulus.

Note that for hot dry air blowing over a cooler sea surface $\Delta\theta > 0$, $\Delta e_p < 0$. The relative importance of humidity and temperature gradients can be seen from the ratio $R = (b\,\Delta e_p) / (\Delta\theta\, p_o)$.

Assuming $p_o = 1000$ mbar

$$R = 4.8\,\Delta e_p / \Delta\theta \simeq 4.8\, s\, \Delta T_s / \Delta\theta \ .$$

$s \sim 0(1)$ mb/^oC and if $\Delta T_s \sim 0(\Delta\theta)$, it can be seen that the influence of humidity and temperature gradients can be of the same order for advective ducts, but that the drier the initial air the more important ΔT_s will be.

$$\text{Now } M(z) = \begin{cases} \Phi_1 + S\left(1 - (z/h)^{1/4}\right) + 0.13z \ , & z < h \\ \Phi_1 + 0.13z \ , & z > h \end{cases} \qquad \ldots.(11)$$

where $S = \dfrac{c}{\theta_1^2}\,(p_o \Delta\theta - b\,\Delta e_p)$.

So that $$\frac{\partial M}{\partial z} = -\frac{1}{4}\left(S(z/h)^{-3/4} / h\right) + 0.13 \ , \qquad z < h \ .$$

The height of the radar duct, z_D , is the height where $\dfrac{\partial M}{\partial z} = 0$, and from the above equation this is at

$$z_D = \left(\frac{S}{0.52}\right)^{4/3} h^{-1/3} \qquad \ldots.(12)$$

provided $z_D < h$. Duct height is at $z = h$, if z_D from equation (12) is greater than h , or in other words, equation (12) holds for $h > (S/0.52)$. Note that from equation (12) z_D decreases as h (and fetch) increases. From equation (6)

$$h = 1.40 \times 10^{-2} \times \left(\frac{g' x}{u^2}\right)^{-0.47} \ .$$

Therefore equation (12) becomes

$$z_D = (S/0.52)^{4/3}\left(1.46 \times 10^{-2} \times \left(\frac{g' x}{u^2}\right)^{-0.47}\right)^{-1/3}$$

$$= 9.78\, S^{4/3} (g'/u^2)^{0.16}\, x^{-0.18}$$

Note that z_D decreases slowly with fetch. (The units in the equations of this section are S.I. apart from those for p_o and water vapour pressures which are in mb.)

The forms of modified refractive index profiles, using equation (11), for $S = 30$, which is a typical value, are shown in fig 7 for a number of values of h. The M profile for homongeneous air and the locus of z_D are shown as dashed lines.

It can be seen here how the depth of the duct, which equals h for shorter fetches, increases till $h = (S/0.52)$, and subsequently decreases with fetch. Note that for $z_D < z < h$ the gradient of refractive modulus is reduced below that for a homogeneous atmosphere so that the radar range to elevated targets is thereby increased even for targets well above the duct.

A measure of duct strength can be obtained by computing the number of modes, m, trapped in the duct as if the refractive modulus were a function of height only. This is given (Kerr, 1951) approximately by

$$m = \frac{2\sqrt{2} \times 10^{-3}}{\lambda} \int_0^{z_D} \left(M(z) - M(z_D) \right)^{\frac{1}{2}} dz + \frac{1}{4} ,$$

where λ = radar wave-length.

m has been calculated for modified layer depths between 20 and 200 m, for $S = 10$, 30 and 50, for $\lambda = 3$ cm and 12 cm (corresponding to X band and S band radars, respectively). The results are presented in figs 8 ($\lambda = 3$ m) and 9 ($\lambda = 12$ cm). It can be seen that S has more effect than h on the number of trapped modes, and that more are trapped for $\lambda = 3$ cm than for $\lambda = 12$ cm. This means that although radar ranges with a smooth sea surface may be greater for 3 cm radar the amount of interference and consequent fading will also be greater at 3 cm. If the sea surface is rough, the propagation in the duct at 3 cm will sometimes be weaker than at 12 cm. The in-duct attenuation in dB/km due to surface scattering $\propto \left(\frac{\text{surface roughness}}{\lambda} \right)^{\frac{1}{2}}$. From Craig (1946) S is typically between 30 and 40 so that the one or two trapped modes for $\lambda = 12$ cm at these S values, should give good propagation. If $m = 1$ exactly, the horizontal damping is of the order of 1 dB/km. As m increases, the damping decreases.

4. FORECASTING OF ADVECTIVE DUCTS

From the previous section it was seen that the important parameter determining strength of the radar duct was S given by

$$S = \frac{c}{\theta_1^2} (p.\Delta\theta - b\Delta e_p) \quad . \qquad \ldots.(13)$$

To determine whether or not a surface based advective duct will occur at a particular time one needs to know the wind-direction (off-shore, on-shore or parallel to the coast) and the sign of $\frac{\Delta\rho}{\rho}$. The actual value of $\left(\frac{g\Delta\rho}{\rho u^2}\right)$ which determines h(x) is not quite so important. From section 2

$$\frac{\Delta\rho}{\rho} = -\frac{\Delta\theta}{\theta_1} - \frac{3\Delta e_p}{8p_o} \qquad \ldots.(14)$$

Hence the important quantities for forcecasting advective radar ducting and for climatological studies are the changes in potential temperature and potential water vapour pressure between the well-mixed upstream air and that in the thermodynamic equilibrium at the sea surface. The climatology of advective radar ducting will be examined in a future report.

Acknowledgements

Thanks are due to Dr. M. Hall for his advice on the radar propagation calculations.

REFERENCES

1. Craig, R.A. (1946). "Measurements of temperature and humidity in the lowest 1000 feet of the atmosphere over Massachusetts Bay". Papers in Physical Oceanography and Meteorology, published by Mass. Inst. of Tech. and Woods Hole Oceanog. Inst. vol x, No. 1 pp 6-47.

2. Craig, R.A. (1949). "Vertical eddy transfer of heat and water vapour in stable air". J. Meteorology 6, 123-133.

3. Kerr, D.E. (1951) "Propagation of short radio waves. McGraw-Hill, New York.

4. Lane, J.A., T. Laevastu, J. Richter, J. Rosenthal, and S. Wickerts (1976). NATO Science Committee. Special Programme Panel of Radio Meteorology Working Group Report on Atmospheric Ducts and Radio-Wave Propagation.

TABLE 1

Figure No.*	x (Km)	h (m)	U m/sec	$\Delta\theta$ (^{o}C)	$-\Delta T_s$ (^{o}C)	$\frac{g'x}{U^2}$	Inversion below 300 m
K 33	45.1	152	11.2	3.9	8.7	34.7	
K 34	48.3	61	6.7	4.7	7.8	141.0	✓
K 35	33.8	91	9.4	4.9	8.3	50.7	
K 36	14.5	61-91	15.6	6.0	6.9	10.9	
K 37	37.0	91	15.6	6.1	7.7	28.2	
K 38	12.9	61	17.9	8.5	0.2	11.5	
K 16	57.9	91	6.7	6.4	-3.5	301.0	
K 19	4.8	31-46	8.0	9.4	9.1	22.0	
K 14	41.8	91	9.8	3.6	6.7	41.8	✓
C 20	3.2	15	8.0	10.0	-2.2	17.4	✓
C 25	19.3	61	15.6	6.6	5.8	17.0	
C 26	4.8	30.5	8.9	9.4	2.2	19.8	
C 31	16.1	61-76	9.4	4.4	6.7	22.5	
C 36	12.9	31-46	8.9	6.7	7.8	33.5	
C 37	38.6	91	9.8	5.0	8.9	54.1	
C 38	77.2	122-213	11.2	3.1	5.3	54.8	
C 39	107.8	122-274	11.2	3.3	5.0	81.9	
C 42	48.3	15	6.7	3.9	2.2	13.0	✓
C 43	20.9	61-91	6.7	3.3	2.2	48.1	✓
C 44	40.2	91-122	6.7	3.3	2.2	92.5	✓
C 7	3.2	30-61	13.4	7.2	6.1	4.2	

* Experiments are designated by their figure number in Kerr (1951) or Craig (1946).

e.g. K 36 denotes Fig. 3.36 of Kerr (1951)

C 20 denotes Fig. 20 of Craig (1946)

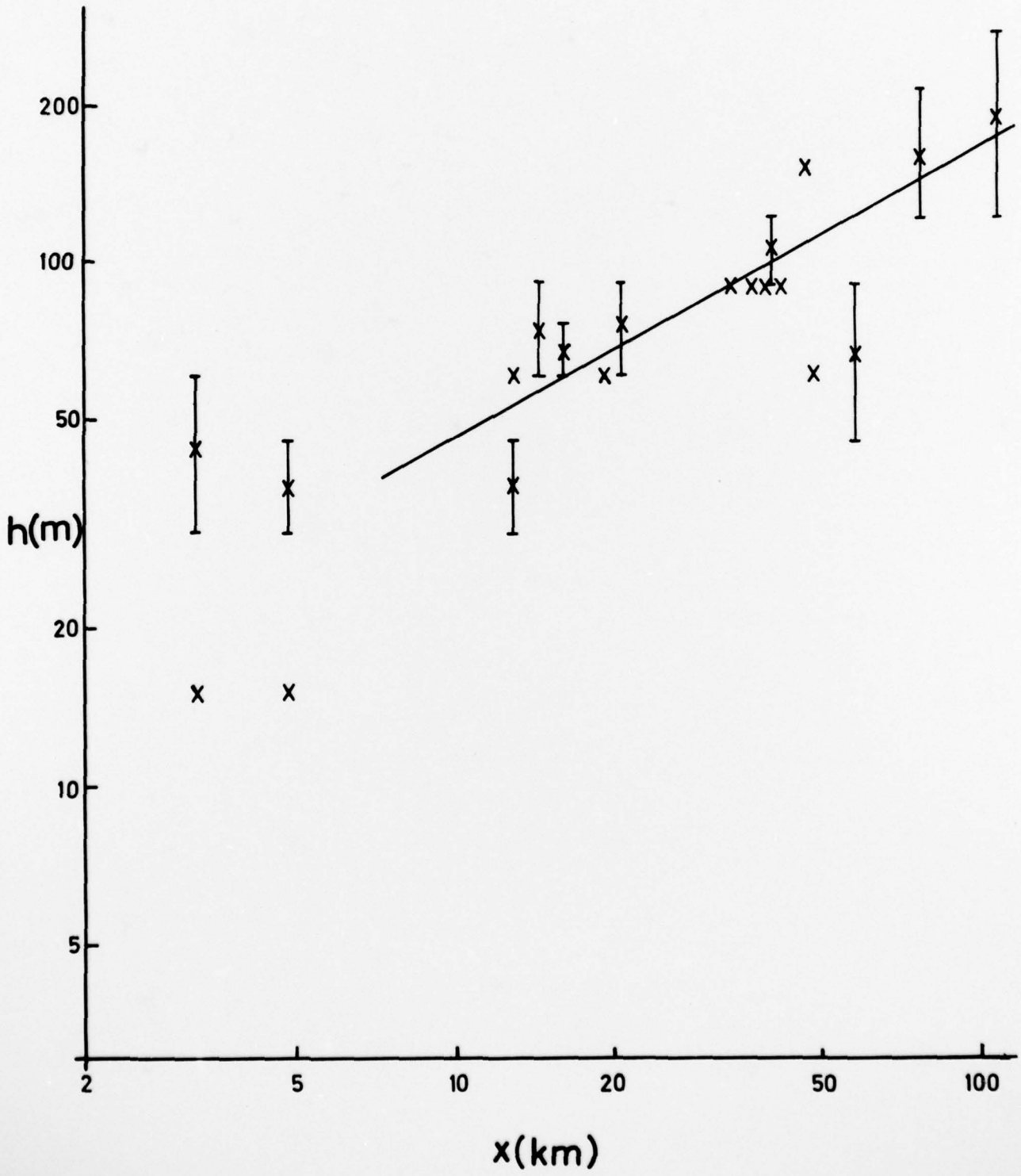

Figure 1. Growth of modified layer with fetch

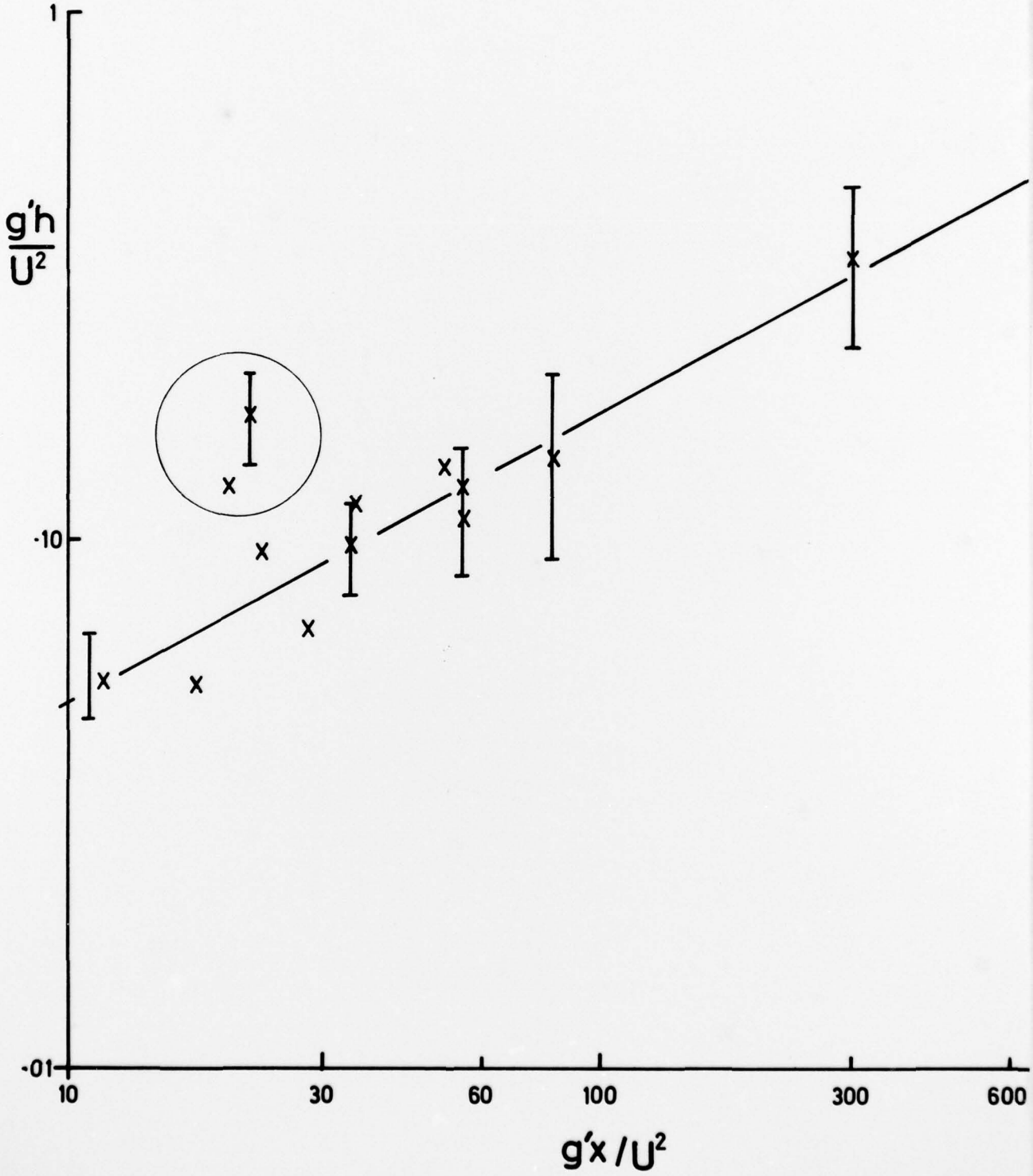

Figure 2. Non-dimensional layer height as a function of non-dimensional fetch

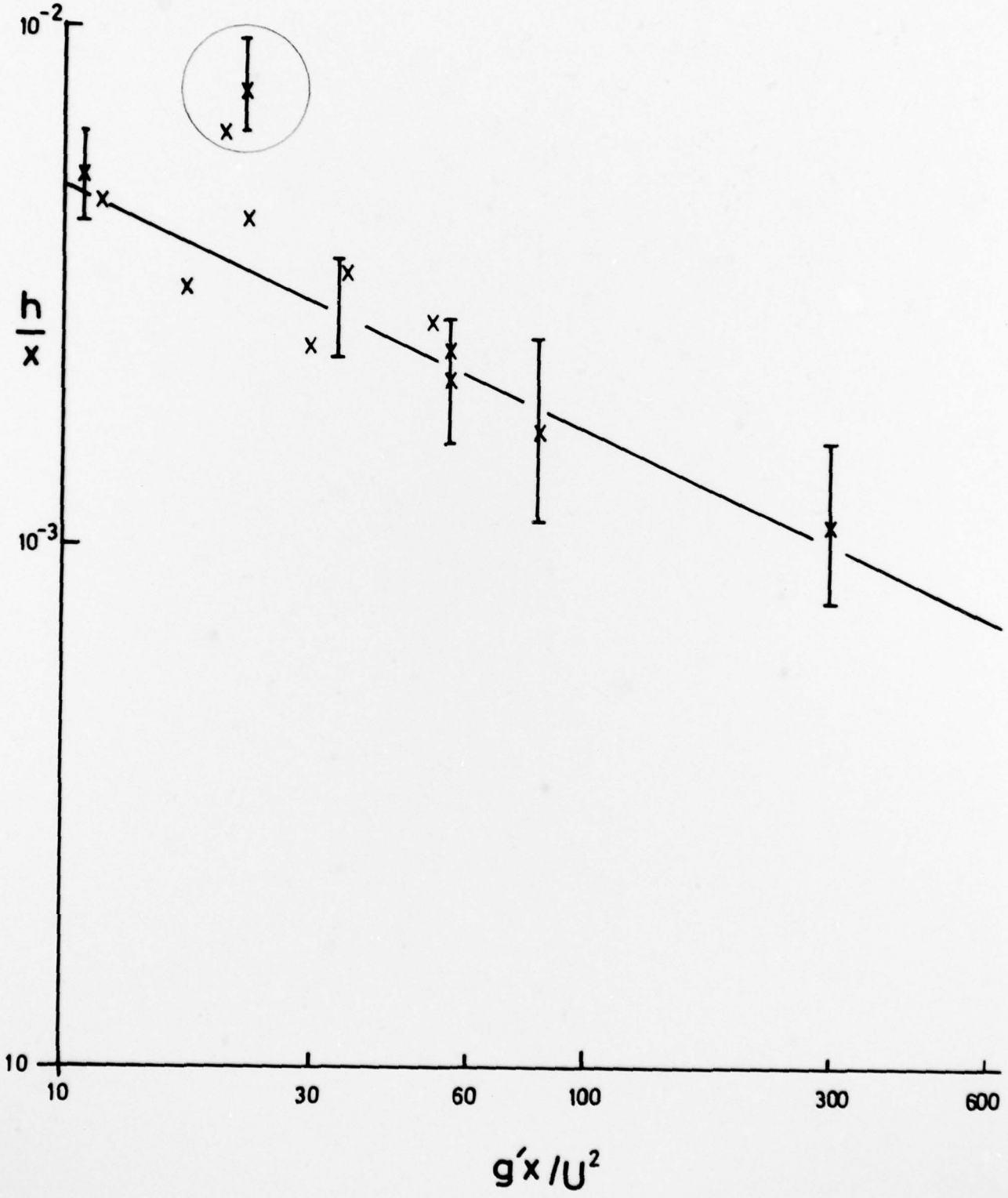

Figure 3. Ratio of layer height to fetch as a function of non-dimensional fetch

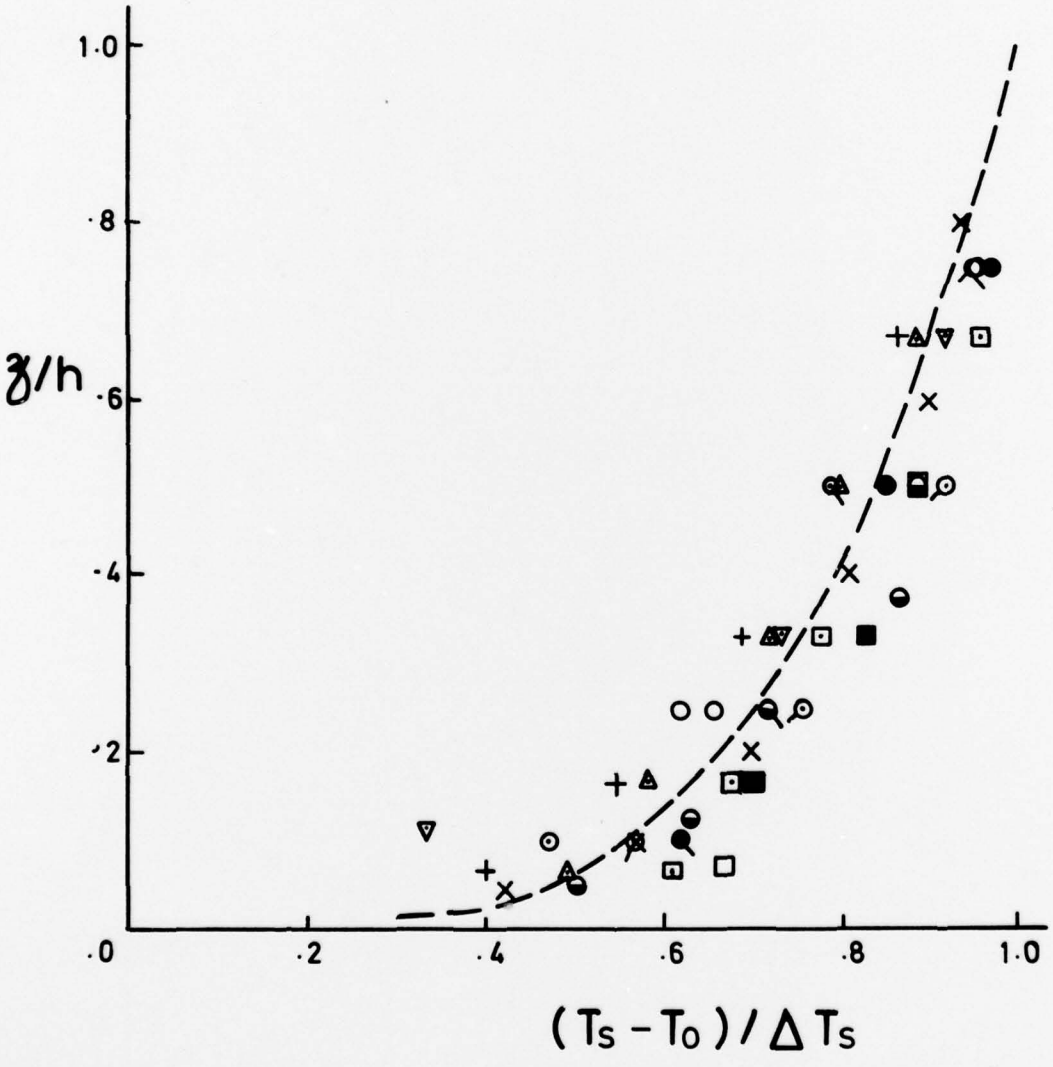

Figure 4. Non-dimensional potential dew point profiles for $x \geq 16$ km. Symbols denote data from Figures of Kerr (1951) or Craig (1946) as described in footnote to Table 1.
●, C25; ⊡, C37; ⊙, C43; ⊙, C44; ◒, K37; x, K33; ⊙, K34; +, K35; △, K14; ▽, K16; ■, C31.
Dashed line is $(z/h)^{\frac{1}{4}}$.

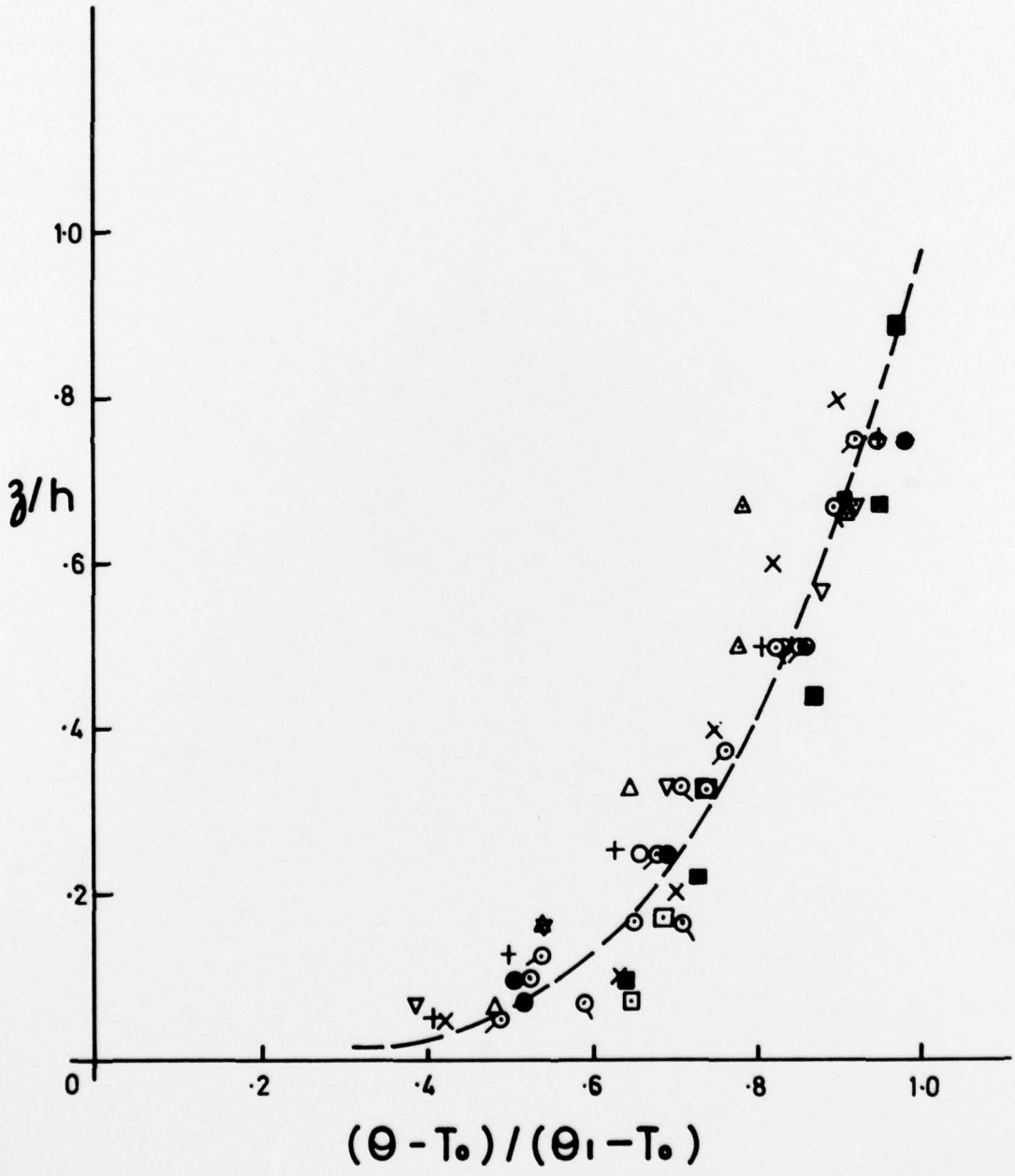

Figure 5. Non-dimensional potential temperature profiles for x ≥ 16 km. Symbols as in Figure 4.

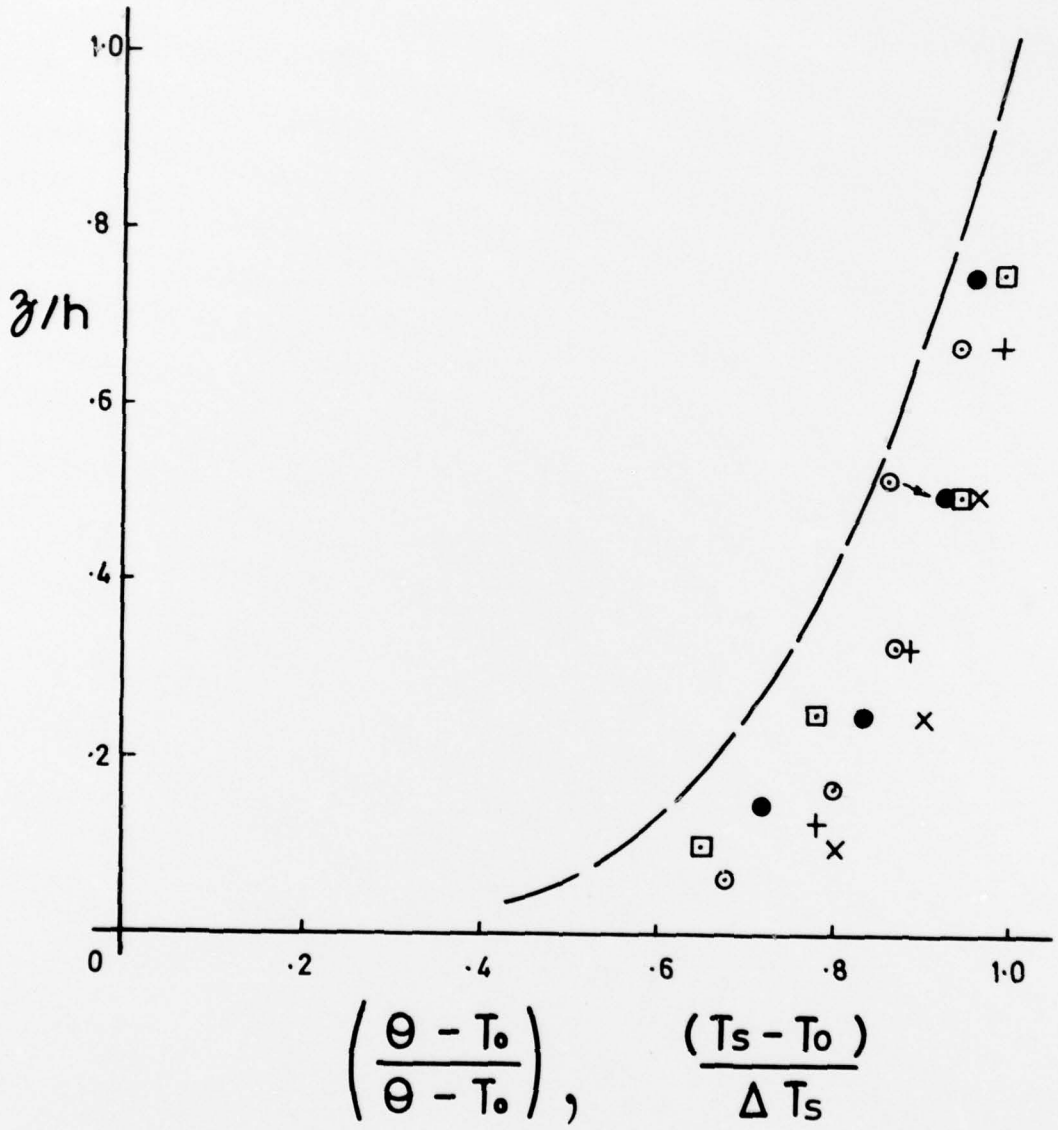

Figure 6. Non-dimensional potential dew point and temperature profiles for $12.8 \leq x \leq 16$ km.

Temperatures: x, C36; ●, K36; ⊡, K38
Dew-Point +, C36; ⊙, K36.

Dashed line is $(z/h)^{\frac{1}{4}}$.

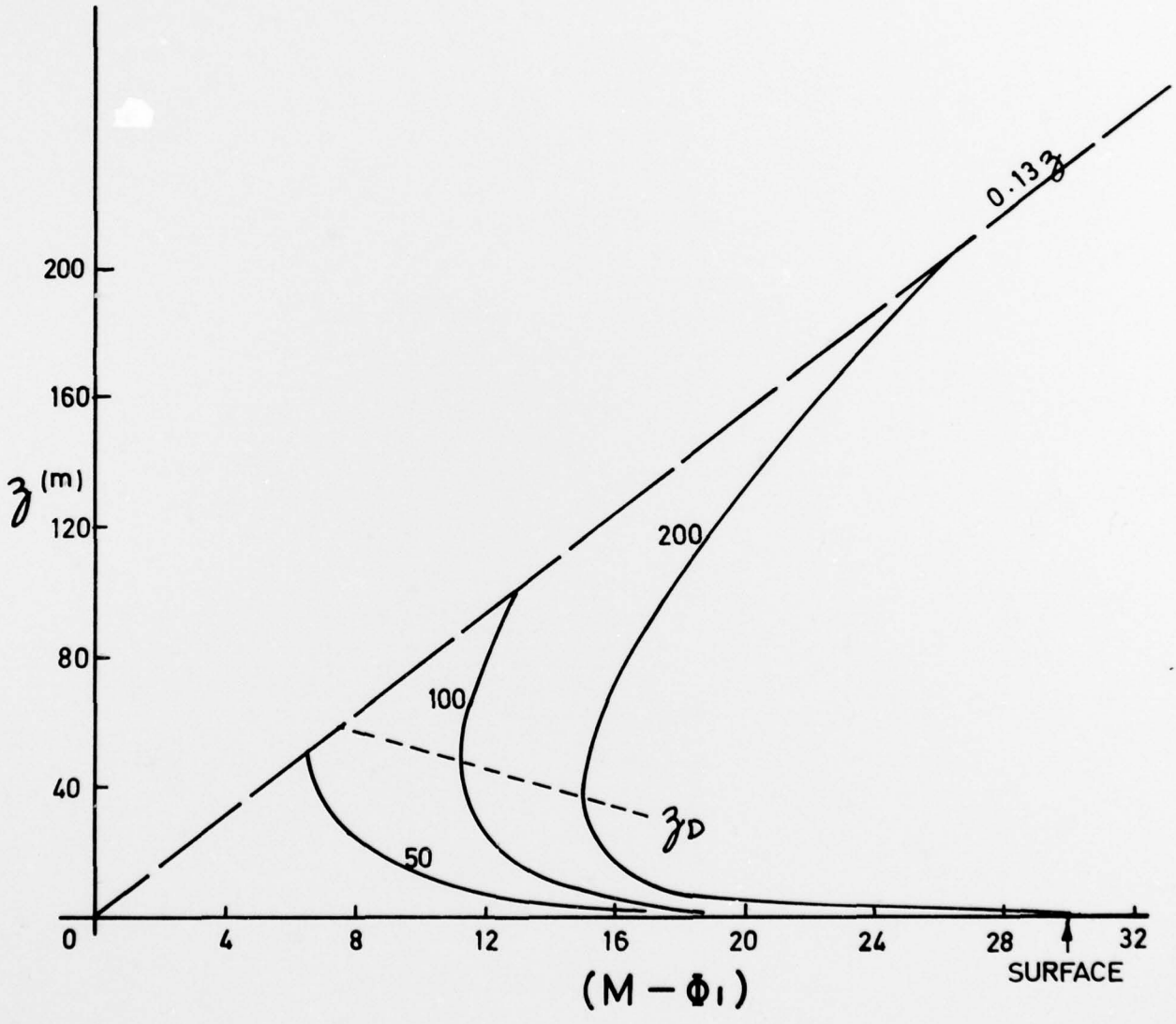

Figure 7. Refractive modulus profiles for S = 30, h = 50, 100, 200 m. Long-dashed line is profile for a homogeneous atmosphere Short-dashed curve is locus of z_D.

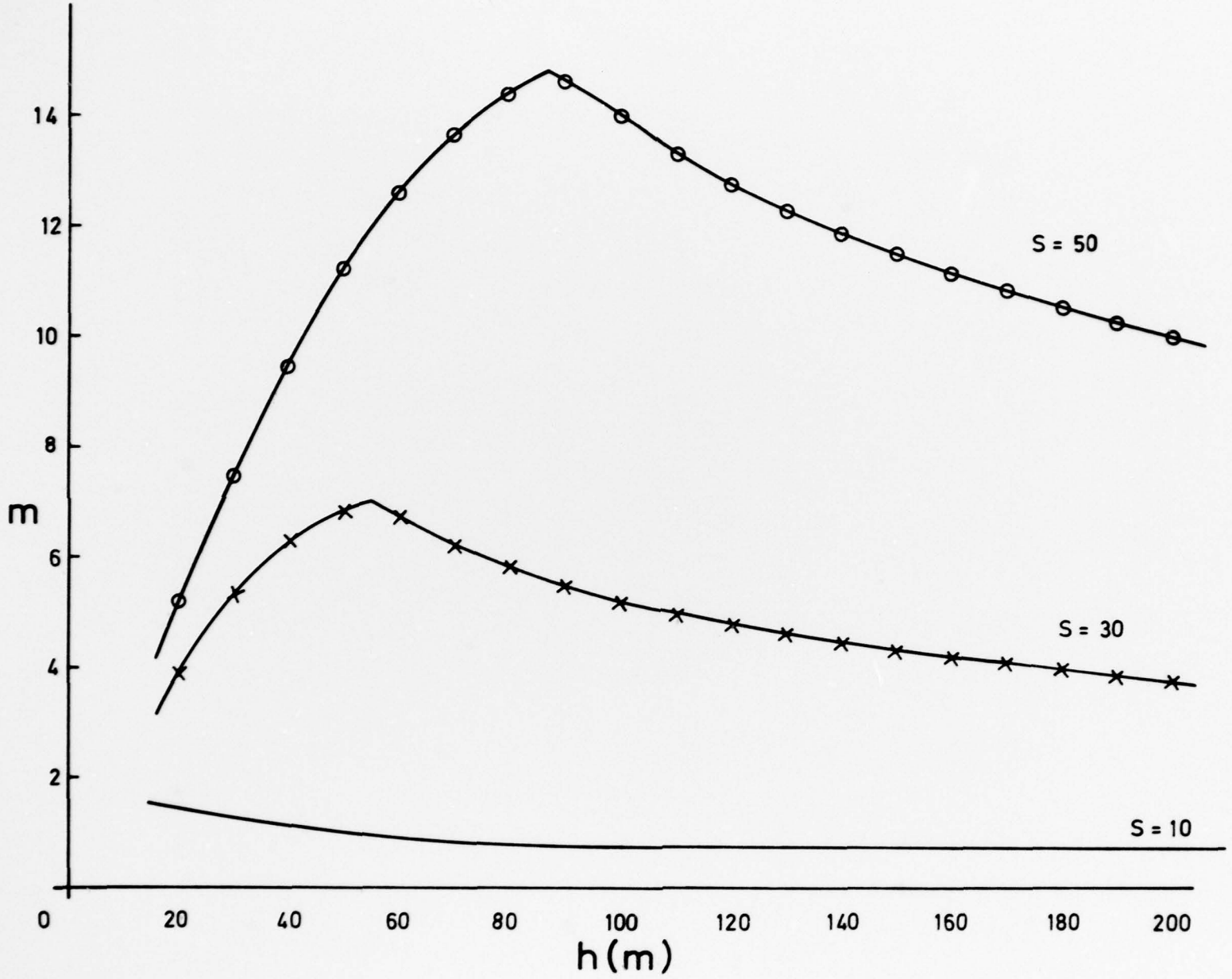

Figure 8. Number of trapped modes for a 3 cm radar as a function of modified layer depth and of S.

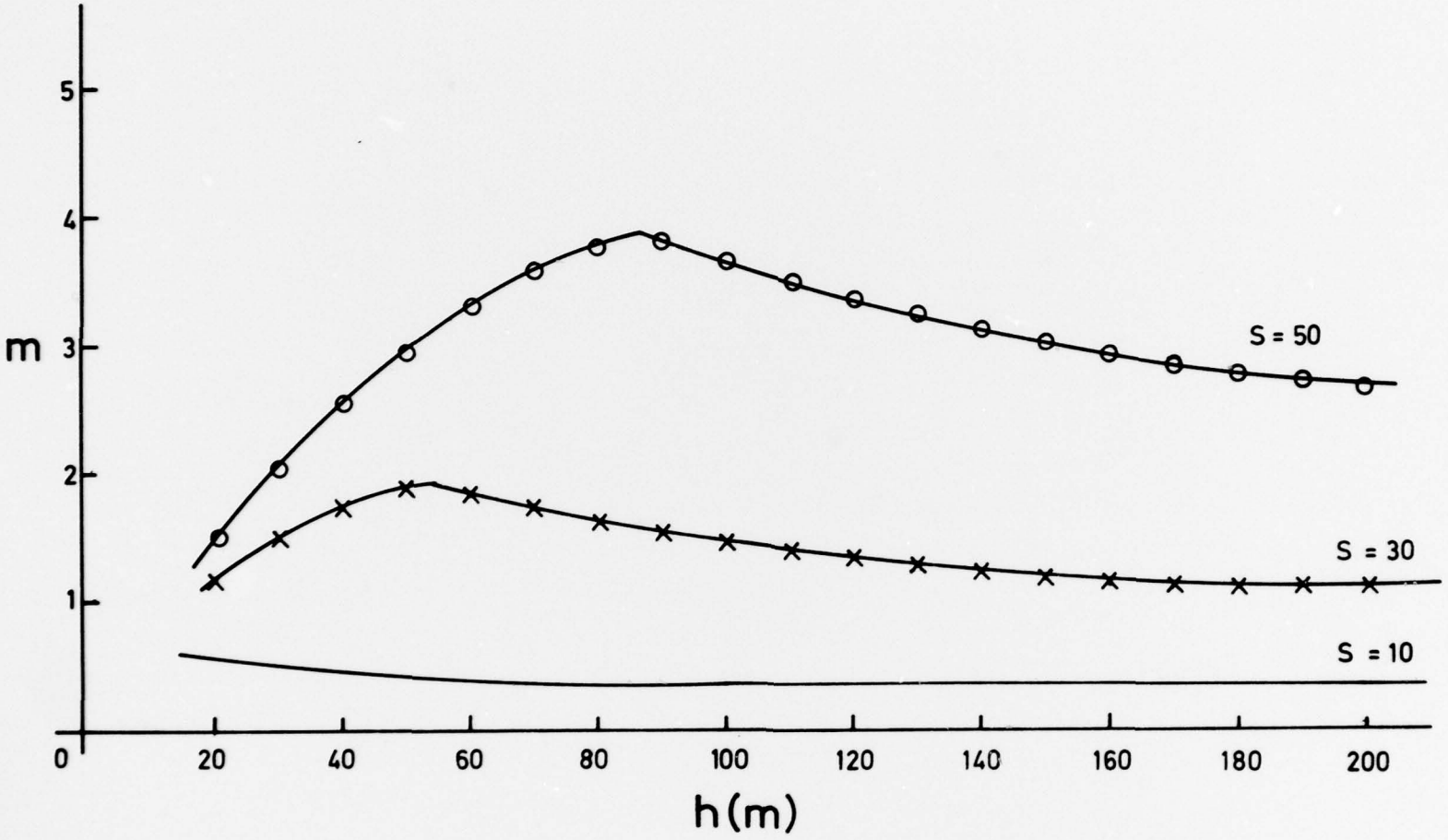

Figure 9. Number of trapped modes for a 12 cm radar as a function of modified layer depth and of S .